Hindawi
Journal of Nanomaterials
Volume 2017, Article ID 1404328, 8 pages
https://doi.org/10.1155/2017/1404328

Research Article

Self-Assembly of 3D Fennel-Like Co_3O_4 with Thirty-Six Surfaces for High Performance Supercapacitor

Yanfang Li,[1] Zhenyin Hai,[2] Xiaojuan Hou,[1] Hongyan Xu,[3] Zengxing Zhang,[1] Danfeng Cui,[1] Chenyang Xue,[1] and Binzhen Zhang[1]

[1]*Science and Technology on Electronic Test and Measurement Laboratory, North University of China, Taiyuan, Shanxi 030051, China*
[2]*Department of Applied Analytical & Physical Chemistry, Ghent University, Global Campus, 119 Songdomunhwa-ro, Yeonsu-gu, Incheon 21985, Republic of Korea*
[3]*School of Materials Science and Engineering, North University of China, Taiyuan, Shanxi 030051, China*

Correspondence should be addressed to Chenyang Xue; xuechenyang@nuc.edu.cn

Received 1 December 2016; Accepted 2 February 2017; Published 7 March 2017

Academic Editor: Nicholas Roberts

Three-dimensional (3D) fennel-like cobalt oxide (II, III) (Co_3O_4) particles with thirty-six surfaces on nickel foams were prepared via a simple hydrothermal synthesis method and its growth process was also researched. The crystalline structure and morphology were investigated by X-ray diffraction (XRD), scanning electron microscopy (SEM), and Raman spectroscopy. The Brunauer-Emmett-Teller (BET) analysis revealed that 3D fennel-like Co_3O_4 particles have high specific surface area. Therefore, the special structure with thirty-six surfaces indicates the good electrochemical performance of the micron-nanometer material as electrode material for supercapacitors. The cyclic voltammetry (CV), galvanostatic charge-discharge, and electrochemical impedance spectroscopy (EIS) were conducted to evaluate the electrochemical performances. Compared with other morphological materials of the similar sizes, the Co_3O_4 particles on nickel foam exhibit a high specific capacitance of 384.375 $F{\cdot}g^{-1}$ at the current density of 3 $A{\cdot}g^{-1}$ and excellent cycling stability of a capacitance retention of 96.54% after 1500 galvanostatic charge-discharge cycles in 6 M potassium hydroxide (KOH) electrolyte.

1. Introduction

To alleviate the energy crisis and greenhouse pollution derived from excessive consumption of fossil fuels, the research on alternative energy conversion and storage systems is urgently called for. Supercapacitors, also known as electrochemical capacitors or ultracapacitors, are a new type of energy storage device, which is considered to be the most promising component [1, 2]. It has a high power density, short charging time, long cycling life, better safety, and environment protection features [3, 4]. According to the energy storage mechanism, supercapacitors are divided into double layer and Faradic capacitor [5, 6]. The Faradic pseudocapacitor with high energy density characteristics receives much concern. Amongst the transition metal oxides which have typical characteristics of Faradic capacitor, Co_3O_4 is one of the most widely exploited and researched oxides due to its importance for various scientific technologies and rich natural resources of Co element [7, 8].

Co_3O_4 with a typical spinel structure and characteristics of simple synthesis, low cost and environment-friendly, has many functional applications, including sensors [9], catalysts [10], and lithium ion batteries [11]. As an electrode material of supercapacitors, Co_3O_4 has excellent electroactivity with extremely high theoretical capacitance of 3560 $F{\cdot}g^{-1}$ [12]. The research showed that the size, morphology, and microstructure of Co_3O_4 particles have significant impacts on physical and electrochemical properties [13]. The Co_3O_4 particles with hollow nanospheres [14], hexagonal tablets [15], octahedral [16], and other structures have been synthesized via different processes, and various were assembled by those units [17, 18]. However, many of them have low specific capacitance or poor cycling stability as the working electrodes [19, 20].

Herein, three-dimensional (3D) symmetrical fennel-like Co_3O_4 particles with thirty-six surfaces on nickel foam were prepared via a simple hydrothermal synthesis method. The crystalline structure and morphology were investigated by XRD, BET, SEM, and Raman spectroscopy. The test of electrochemical characteristics showed that Co_3O_4 particles on nickel foam exhibit a good specific capacitance of 384.375 $F \cdot g^{-1}$ at the current density of 3 $A \cdot g^{-1}$. The specific capacitance after 1500 cycles still remains about 96.54%. This demonstrates that the fennel-like Co_3O_4 particles show excellent long-term electrochemical stability as an electrode material for supercapacitors.

2. Experimental

2.1. Preparation of the 3D Fennel-Like Co_3O_4. 3D fennel-like Co_3O_4 was synthesized by hydrothermal method. Nickel foams were preprocessed by acetone and 3 mol/L hydrochloric acid. The ammonium fluoride was supplied by Tianjin Guangfu Technoligy Development Co. Ltd. The potassium hydroxide, urea, and cobalt (II) chloride hexahydrate were obtained from Sinopharm Chemical Reagent Co. Ltd. All those materials are analytical grade. 1 mmol cobalt (II) chloride hexahydrate ($CoCl_2 \cdot 6(H_2O)$), 3 mmol urea ($CO(NH_2)_2$), and 7.5 mmol ammonium fluoride (NH_4F) were dissolved in 30 ml deionized water with magnetic stirring 15 min. The same configured solutions were obtained by repeating the above experimental procedure. Then the configured solutions were put into 50 ml Teflon reactors with the pretreatment nickel foams as substrate, respectively. The reactions were sustained 5 h and 12 h at 120°C in electric drying oven, respectively. After the reaction, the nickel foams with precursors were cleaned twice via ultrasonic using deionized water and then dried 6 h at 60°C. The precursors on nickel foams were roasted 2 h at 400°C in three-zone tube furnace (OTF-1200X-60 -III) to get Co_3O_4 crystals.

2.2. Characterization of the 3D Fennel-Like Co_3O_4. The morphology was investigated by scanning electron microscopy (SEM, SUPRA 55 SAPPHIRE). The X-ray diffraction (XRD) for analyzing material phase and crystal structure was measured on a Bruker D8 with Cu Kα (λ = 0.15406 nm) radiation at 40 eV in the 2θ of 10~80°. The Raman spectrum (inVia confocal micro-Raman spectroscopy) was used to determine the energy of physical vibration and rotation in order to identify material properties. Nitrogen (N_2) adsorption-desorption isotherm measurements were performed by using the QuadraSorb SI of Quantachrome Instruments at 77.3 K. Before adsorption-desorption isotherm measurements, the samples were outgassed at 300°C for 6 h.

2.3. Electrochemical Performance Measurement. Electrochemical performance measurements were performed on an electrochemical workstation (Instruments, RST5202F) using a three-electrode mood with a platinum foil as counter electrode, a saturated calomel electrode (SCE) as the reference electrode, and the 3D fennel-like Co_3O_4 on nickel foam directly used as working electrode in 6 mol/L KOH aqueous solution. Cyclic voltammetry (CV) was performed in the potential window from 0 to 0.55 V at various scan rates (0.001 $V \cdot s^{-1}$, 0.005 $V \cdot s^{-1}$, 0.01 $V \cdot s^{-1}$, 0.03 $V \cdot s^{-1}$, and 0.05 $V \cdot s^{-1}$). Galvanostatic charge-discharge measurements were carried out with the potential range from 0 to 0.4 V at specific current densities ranging from 3 $A \cdot g^{-1}$ to 21 $A \cdot g^{-1}$. Electrochemical impedance spectroscopy (EIS) test was performed in the frequency range from 1 kHz to 1.0 Hz.

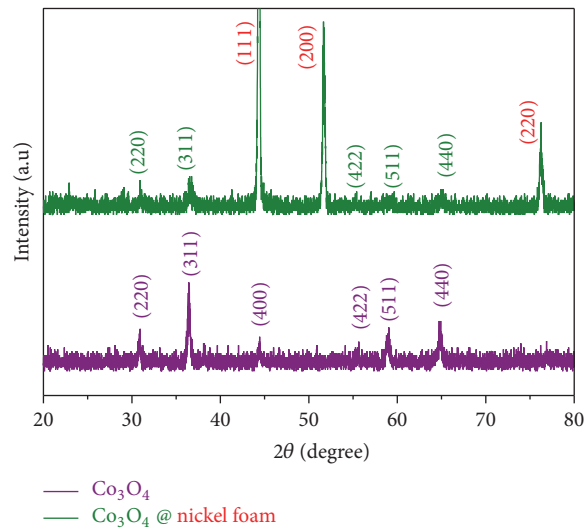

FIGURE 1: XRD patterns of Co_3O_4 @ nickel foam and Co_3O_4 particles peeled off from nickel foam.

3. Results and Discussion

3.1. The Structure of 3D Fennel-Like Co_3O_4. The XRD pattern is showed in Figure 1, which is used to examine the crystalline structure of the prepared 3D fennel-like Co_3O_4. The green curve of Co_3O_4 on the Ni substrate shows three obvious diffraction peaks of Ni substrate at 2θ = 44.37, 51.59, and 76.08, attributed to (111), (200), and (220), respectively, which agrees well with CPDS card (JCPDS NO. 01-1258). It can be seen that relatively apparent diffraction peaks of Co_3O_4 at 2θ = 31.27, 36.85, 55.66, 59.36, and 65.24 can be attributed to (220), (311), (422), (511), and (440), respectively, which agrees well with CPDS card of the standard spinel cubic Co_3O_4 (JCPDS NO. 42-1467) [27]. Because of the less Co_3O_4 particles covering on nickel foam, the diffraction peaks of Ni are stronger than those of Co_3O_4. From the purple curve of Co_3O_4 particles peeled off from the nickel foam, it can be seen that the diffraction peaks of Co_3O_4 at 2θ = 31.27, 36.85, 44.81, 55.66, 59.36, and 65.24 can be attributed to (220), (311), (400), (422), (511), and (440), respectively. The results demonstrate that the Co_3O_4 particles have a typical spinel structure.

The Raman spectra of 3D fennel-like Co_3O_4 on Ni substrate show characteristic peaks (482 cm^{-1}, 528 cm^{-1}, and 686 cm^{-1}) of Co_3O_4 in Figure 2. The strongest peak of Co_3O_4 at 686 cm^{-1} corresponds to symmetric stretching vibration. The two peaks at 482 cm^{-1} and 528 cm^{-1} are the result of the translation motion of oxygen atoms relative to divalent

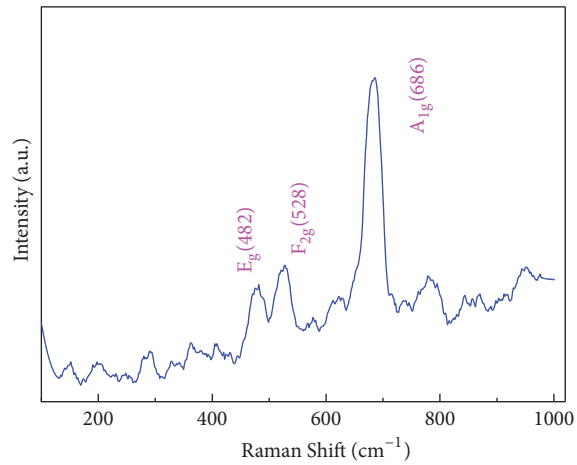

FIGURE 2: Raman spectrum of Co_3O_4.

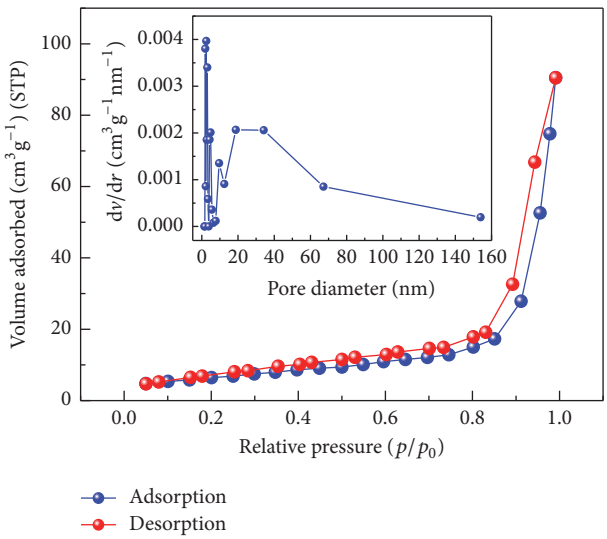

FIGURE 3: N_2 adsorption-desorption isotherm of 3D fennel-like Co_3O_4 (the inset corresponds to pore size distribution).

cations (Co^{2+}), respectively [28, 29]. The other weak peaks are related to the interference of nickel foam substrate.

Additionally, to gain insight into the specific surface area and pore size distribution of 3D fennel-like Co_3O_4, Brunauer-Emmett-Teller (BET) are further performed to examine the specific surface area and pore size distribution. From the N_2 adsorption-desorption isotherm shown in Figure 3, it can be observed that the isotherms show typical IV sorption behavior with a hysteresis loop in the larger range of 0.2~1.0 P/P_0, indicating the existence of mesopores possibly formed by the loose stacking of constituent particles [30]. The corresponding Barrett-Joyner-Halenda (BJH) pore size distribution data (the inset in Figure 3) shows that the pore size is uniform within the range of mesopores. The BET specific area and the BJH desorption pore volumes are 34.99 $m^2 \cdot g^{-1}$ and 0.144 $cm^3 \cdot g^{-1}$, respectively. The specific surface area provides numerous electroactive sites for fast and reversible redox reactions between the electrolyte and electroactive species on the electrode surface [31].

3.2. The Surface Morphology of 3D Fennel-Like Co_3O_4. Morphology is a key factor that influences the electrochemical characteristics, where an appropriate morphology and optimized structure will facilitate electrolyte ion transport [32]. The SEM images in Figures 4(a) and 4(b) show the morphology of 3D fennel-like Co_3O_4 (prepared for 12 h at 120°C) at low magnification and high magnification, respectively. It can be seen in Figure 4(a) that Co_3O_4 particles with the uniform size and morphology are covered on nickel foam, and there are many interspaces amongst particles, which plays an important role in improving ratio and dynamic performance of electrode material. It contributes to the filling of electrolyte solution for forming an electrolyte storage buffer, provides protection for the adjacent electrolyte interface diffusion and ion transport, and reduces the diffusion path for electrolyte [33]. Figure 4(b) demonstrates that Co_3O_4 particle is about 5 μm in diameter and has a hexagonal fennel-like morphology with thirty-six surfaces and symmetrical characteristic, which increases the contact area and accelerate the material transport between electrolyte and electrode.

In this study, hydrothermal method was used to provide a special physicochemical condition for the crystallization of precursor reaction and regulate various physical parameters of crystal growth. The growth (restrained or enhanced) of specific crystal plane is influenced by different solvents to affect the crystalline morphology. Thus, NH_4F was used as the solvent. Figures 4(c) and 4(d) are the hexagonal Co_3O_4 particles (prepared for 5 h at 120°C). It can be seen in Figures 4(c) and 4(d) that the surfaces of Co_3O_4 crystal particles are rough, which illustrate that Co_3O_4 has a self-assembly capacity in growth process according to the crystal morphology theory. The rough surface of Co_3O_4 sheet had provided more attachment points for the deposited particles, which made the crystals grow along the steps and superimposed layer by layer [34]. The growth schematic of 3D fennel-like Co_3O_4 particles is illustrated in Figure 5, in which Figure 5(a) is the Co_3O_4 particles prepared for 5 h (T1) at 120°C. Figures 5(b) and 5(c) (T2) correspond to the partial reaction time of preparation of 3D fennel-like Co_3O_4 particles. The total reaction time is 12 h.

3.3. Electrochemical Measurements. Three-electrode test system was used to investigate the pseudocapacitive performance of Co_3O_4 on nickel foam. The cyclic voltammogram (CV) curves of Co_3O_4 on nickel foam were measured under scan rates at 1 to 50 $mV \cdot s^{-1}$ and voltage range from 0 to 0.6 V as shown in Figure 7. However, Figure 6 shows that the signal of nickel foam is quite small, indicating that the capacitance contribution from nickel foam can be negligible. The CV curves in Figure 7 show the pseudocapacitance features caused by the electrochemical reactions. Conversion between different valence states of Co results in two different

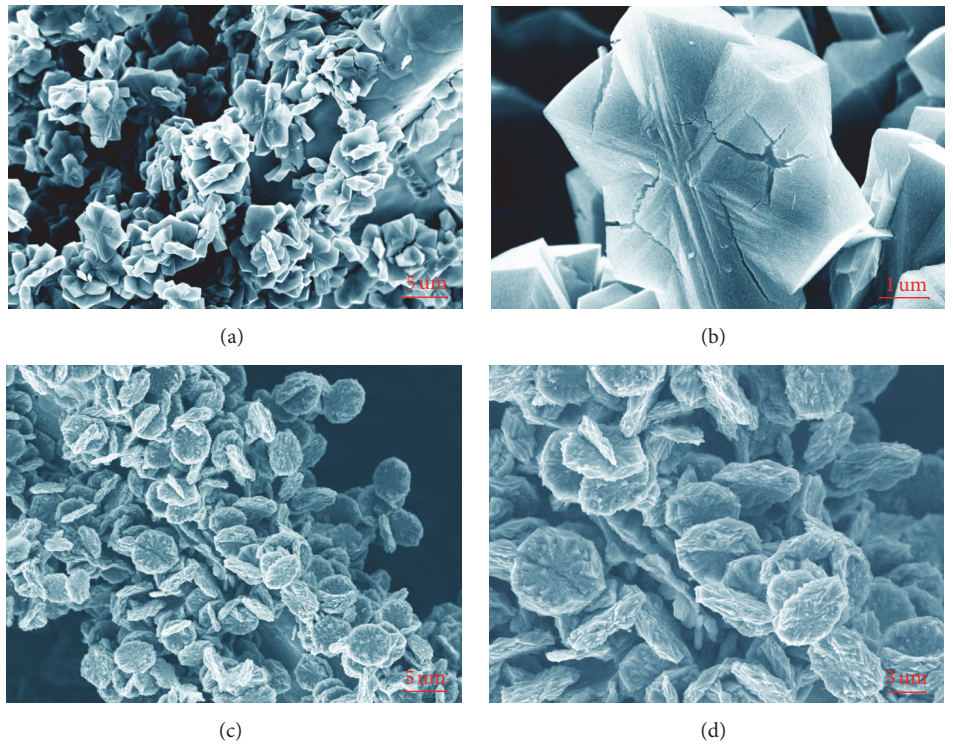

Figure 4: (a) and (b) are the SEM images of 3D fennel-like Co_3O_4 particles (prepared for 12 h at 120°C); (c) and (d) are the hexagonal Co_3O_4 particles (prepared for 5 h at 120°C).

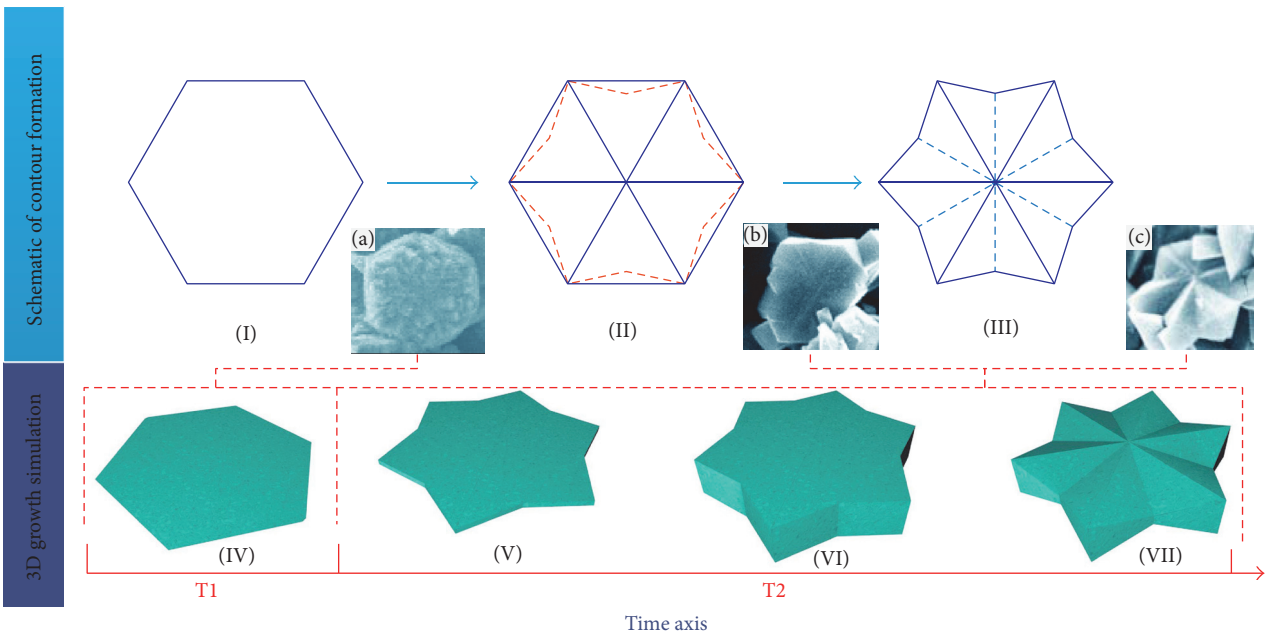

Figure 5: The growth schematic of crystal (I, II, and III are contour forming schematic; IV, V, VI, and VII are 3D growth simulation with two time periods; V, VI, and VII are simultaneous), a is the Co_3O_4 particles prepared for 5 h at 120°C; (b) and (c) are prepared for 12 h at 120°C.

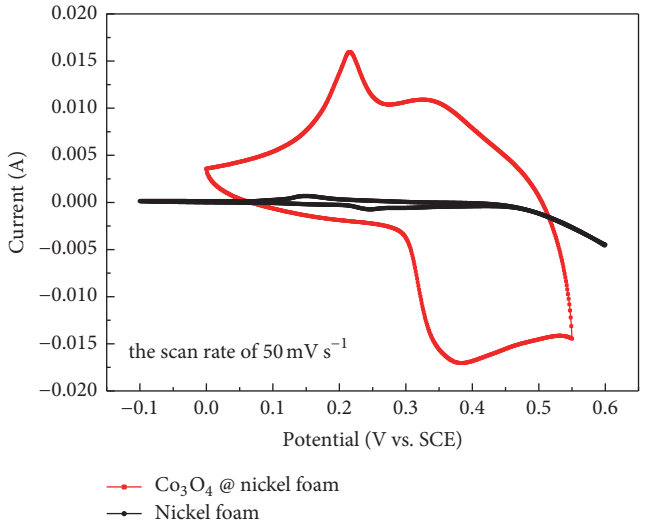

FIGURE 6: CV curves of the Co_3O_4 electrode at a scan rate of 50 mV s^{-1}.

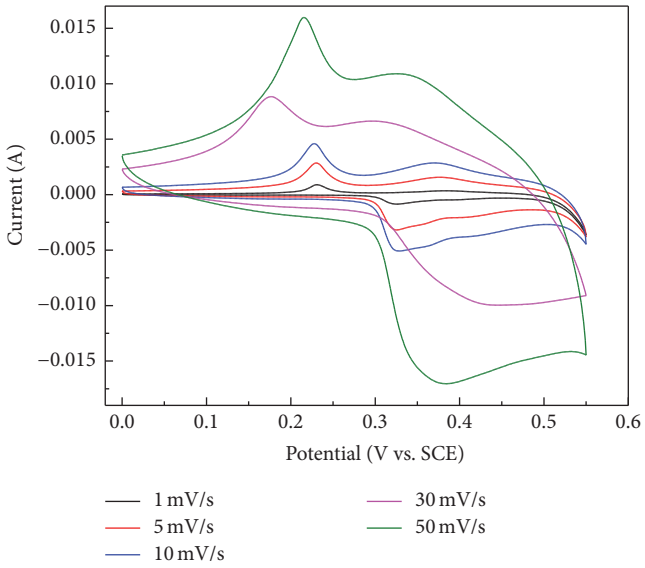

FIGURE 7: CV curves of the Co_3O_4 electrode at different scan rates.

redox peaks. The faradaic reactions can be described by the following formulas [27]:

$$Co_3O_4 + OH^- + H_2O \longleftrightarrow 3CoOOH + e^- \quad (1)$$

$$CoOOH + OH^- \longleftrightarrow CoO_2 + H_2O + e^-. \quad (2)$$

Due to the polarization of electrodes, the anodic and cathodic peaks moved toward the positive and negative directions of voltage with the increase of scan rate, respectively [35]. Considering that the electrolyte is KOH aqueous solution, the electrode reaction of Co_3O_4 is mainly about the embedding and extraction of OH^- [36]. Meanwhile, with increase of scan rate, the capacitor current density increased

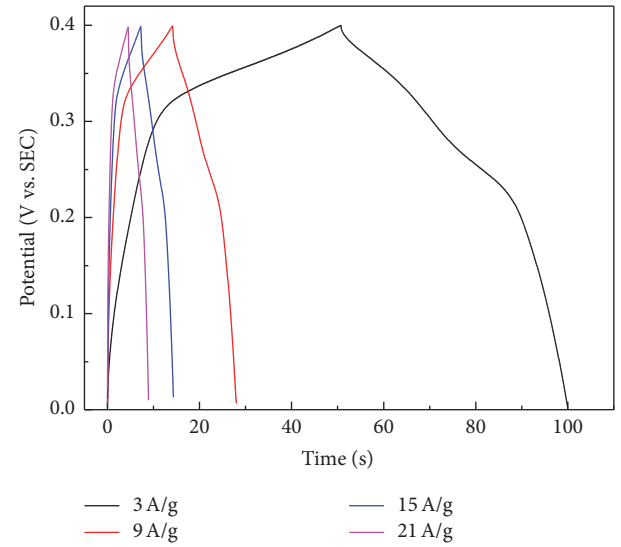

FIGURE 8: Galvanostatic charge-discharge curves of the Co_3O_4 electrode recorded at different current densities.

and the redox peaks were still distinct, indicting a good reversibility of the rapid charge-discharge process of fennel-like Co_3O_4 [27].

The galvanostatic charge-discharge characteristics of Co_3O_4 electrode under different current densities in Figure 8 are consistent with the results of CV measurements. Two pairs of charge and discharge plateaus are well observed at current densities of 3 A·g^{-1}, corresponding to the redox peaks in the CV curves. The specific capacitance of the electrodes can be calculated using the following equation [37]:

$$C_s = \frac{I \cdot t}{m \cdot \Delta V}, \quad (3)$$

where C_s, I, t, m, and ΔV are the specific capacitance of the electrodes (F·g^{-1}), discharging current (A), discharging time (s), mass of the active material (g), and the potential drop (V) during discharging, respectively. The specific capacitances of 3D fennel-like Co_3O_4 electrode are 384.375 F·g^{-1}, 325.781 F·g^{-1}, 277.343 F·g^{-1}, and 240.625 F·g^{-1} at current densities of 3 A·g^{-1}, 9 A·g^{-1}, 15 A·g^{-1}, and 21 A·g^{-1}, respectively. It is more than the specific capacitances of some nanostructures (particulates [21], nanowires [22], nanorods [24], nanotube [25], and sheets [26]) and microstructures (crater-like [19], octahedron [23]).

The electrochemical impedance spectroscopy (EIS) of 3D fennel-like Co_3O_4 electrode is shown in Figure 9. The Nyquist plot shows that EIS is divided into two stages: high and low frequency ranges. Insets show the Nyquist plot in high frequency region (inset (a)) and the equivalent circuit diagram (inset (b)). The solution resistance (R_s) between the counter electrode and working electrode, which includes the electrolyte resistance [38], is about 1.38 Ω estimated from the intercept on the real axis in the high frequency range [19]. R_{po} is the polarization resistance at the surface of electrode.

Table 1: Comparison of the electrochemical performances of Co_3O_4 between literature and this study.

Morphology	Crystal size (Diameter)	Maximum C_s ($F \cdot g^{-1}$)	Capacitance retention	Ref.
Crater-like	0.5~1 μm	102	74% (after 500 cycles)	[19]
Particulates	10~50 nm	162	72.2% (after 1000 cycles)	[21]
Nanowires	20~40 nm	163	98% (after 1000 cycles)	[22]
Octahedron	±1.3 μm	182	99%(after 1000 cycles)	[23]
Nanorods	50~100 nm	202.5	99% (after 1000 cycles)	[24]
Nanotube	5~10 nm	273	88% (after 500 cycles)	[25]
Sheets	100–500 nm	357	87% (after 1000 cycles)	[26]
Bundle-like	±7.9 μm	390.4	95% (after 1000 cycles)	[20]
Fennel-like	4-5 μm	384.38	96.54% (after 1000 cycles)	This study

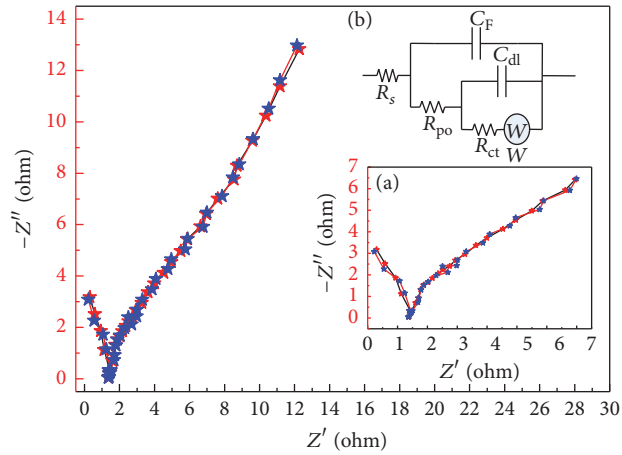

Figure 9: Nyquist plot of the Co_3O_4 electrode, in which the red and blue circles are EIS plot and fitted data, respectively (the inset (a) shows the Nyquist plot of the sample in high frequency and (b) is the equivalent circuit diagram).

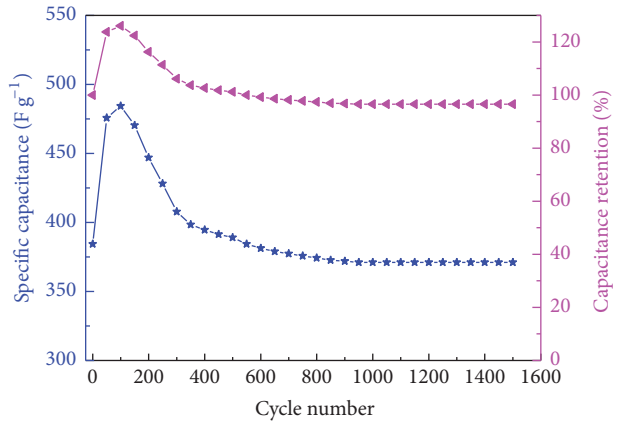

Figure 10: Cycling performance of the Co_3O_4 electrode (at constant current density of 3 $A \cdot g^{-1}$).

C_{dl} and C_f are double layer capacitance and faradaic pseudocapacitance, respectively [39]. The high frequency range of EIS is a curve of large curvature radius, which corresponds to faradaic reaction, and reflects the charge transfer resistance (R_{ct}) controlled by electrochemical reaction kinetics [40]. The straight oblique line in the low frequency range is Warburg impedance (W), which results from the frequency dependence of ion diffusion/transport in the electrolyte. The slope is nearly 1/2, indicating small Warburg impedance and high ion diffusion properties, which result in good electrochemical performance [41].

The cycling stability for Co_3O_4 superstructures is an important quality required for practical applications of the supercapacitors [42]. Figure 10 shows the cycling performance of the Co_3O_4 electrode examined by the galvanostatic charge-discharge tests for 1500 cycles. The initial capacitance is 384.38 $F \cdot g^{-1}$ at current densities of 3 $A \cdot g^{-1}$. It can be seen that at the beginning the specific capacitance increases rapidly until reaching the highest value of 484.4 $F \cdot g^{-1}$ at 100 cycles. Thereafter it drops rapidly and becomes slower after the subsequent 300 cycles. The specific capacitance maintains at 371.1 $F \cdot g^{-1}$ after 900 continuous cycles. Hence, the lowest specific capacitance after 1500 cycles still remains about 96.54% of the initial capacitance (384.38 $F \cdot g^{-1}$). This demonstrates that the 3D fennel-like Co_3O_4 particles show excellent long-term electrochemical stability as an electrode material for supercapacitors.

4. Conclusion

In conclusion, the 3D fennel-like Co_3O_4 particles were synthesized through a simple and mild hydrothermal growth method using nickel foam as a substrate. XRD, Raman spectrum, and SEM results show that Co_3O_4 particles on the Ni substrate have a standard spinel cubic structure with 3D fennel-like. The 3D fennel-like Co_3O_4 particles on Ni substrate are very uniform with the size of 5 μm. As an electrode material for supercapacitors, the electrochemical measurements demonstrate that the 3D fennel-like Co_3O_4 particles exhibit a good specific capacitance of 384.38 $F \cdot g^{-1}$ at current densities of 3 $A \cdot g^{-1}$. The specific capacitance retains about 96.54% after 1500 cycles. Compared with other morphological materials of similar and some smaller size (shown in Table 1), the particles on nickel foam exhibit a high

specific capacitance. The result shows that morphology plays an important role in the electrochemical properties, and the 3D fennel-like Co_3O_4 particles can been a promising material in the application of high performance supercapacitors.

Competing Interests

The authors declare that there is no conflict of interests regarding the publication of this paper.

Acknowledgments

This work was financially supported by the National High-Tech Research and Development (863) Program of China (Grant no. 2015AA042601), the National Science Foundation for Distinguished Young Scholars of China (Grant no. 61525107), and the National Science Foundation of China (Grant no. 61501408).

References

[1] V. Augustyn, P. Simon, and B. Dunn, "Pseudocapacitive oxide materials for high-rate electrochemical energy storage," *Energy and Environmental Science*, vol. 7, no. 5, pp. 1597–1614, 2014.

[2] H. Liu, X. Gou, Y. Wang, X. Du, C. Quan, and T. Qi, "Cauliflower-like Co3O4/three-dimensional graphene composite for high performance supercapacitor applications," *Journal of Nanomaterials*, vol. 2015, Article ID 874245, 9 pages, 2015.

[3] R. N. Reddy and R. G. Reddy, "Sol-gel MnO_2 as an electrode material for electrochemical capacitors," *Journal of Power Sources*, vol. 124, no. 1, pp. 330–337, 2003.

[4] M. Pal, R. Rakshit, A. K. Singh, and K. Mandal, "Ultra high supercapacitance of ultra small Co_3O_4 nanocubes," *Energy*, vol. 103, pp. 481–486, 2016.

[5] B. E. Conway, "Transition from "supercapacitor" to "battery" behavior in electrochemical energy storage," *Journal of the Electrochemical Society*, vol. 138, no. 6, pp. 1539–1548, 1991.

[6] G. Wang, L. Zhang, and J. Zhang, "A review of electrode materials for electrochemical supercapacitors," *Chemical Society Reviews*, vol. 41, no. 2, pp. 797–828, 2012.

[7] J.-W. Lang, L.-B. Kong, W.-J. Wu, Y.-C. Luo, and L. Kang, "Facile approach to prepare loose-packed NiO nano-flakes materials for supercapacitors," *Chemical Communications*, no. 35, pp. 4213–4215, 2008.

[8] V. R. Shinde, S. B. Mahadik, T. P. Gujar, and C. D. Lokhande, "Supercapacitive cobalt oxide (Co_3O_4) thin films by spray pyrolysis," *Applied Surface Science*, vol. 252, no. 20, pp. 7487–7492, 2006.

[9] H. Yamaura, J. Tamaki, K. Moriya, N. Miura, and N. Yamazoe, "Highly selective CO sensor using indium oxide doubly promoted by cobalt oxide and gold," *Journal of the Electrochemical Society*, vol. 144, no. 6, pp. L158–L160, 1997.

[10] F. Švegl, B. Orel, I. Grabec-Švegl, and V. Kaučič, "Characterization of spinel Co_3O_4 and Li-doped Co_3O_4 thin film electrocatalysts prepared by the sol-gel route," *Electrochimica Acta*, vol. 45, no. 25-26, pp. 4359–4371, 2000.

[11] J.-M. Tarascon and M. Armand, "Issues and challenges facing rechargeable lithium batteries," *Nature*, vol. 414, no. 6861, pp. 359–367, 2001.

[12] M. Lindo, A. J. Vizcaíno, J. A. Calles, and A. Carrero, "Ethanol steam reforming on Ni/Al-SBA-15 catalysts: effect of the aluminium content," *International Journal of Hydrogen Energy*, vol. 35, no. 11, pp. 5895–5901, 2010.

[13] T. O. Ely, C. Amiens, B. Chaudret et al., "Synthesis of nickel nanoparticles. influence of aggregation induced by modification of poly(vinylpyrrolidone) chain length on their magnetic properties," *Chemistry of Materials*, vol. 11, no. 3, pp. 526–529, 1999.

[14] G.-G. Yi, Y. Xiao, W.-Q. He et al., "Simple fabrication and electrochemical properties of Co3O4 hollow spheres," *Chinese Journal of Inorganic Chemistry*, vol. 27, no. 1, pp. 162–166, 2011.

[15] D. Su, S. Dou, and G. Wang, "Mesocrystal Co3O4 nanoplatelets as high capacity anode materials for Li-ion batteries," *Nano Research*, vol. 7, no. 5, pp. 794–803, 2014.

[16] X. Wang, L. Yu, X.-L. Wu et al., "Synthesis of single-crystalline Co_3O_4 octahedral cages with tunable surface aperture and their lithium storage properties," *Journal of Physical Chemistry C*, vol. 113, no. 35, pp. 15553–15558, 2009.

[17] X. Qing, S. Liu, K. Huang et al., "Facile synthesis of Co3O4 nanoflowers grown on Ni foam with superior electrochemical performance," *Electrochimica Acta*, vol. 56, no. 14, pp. 4985–4991, 2011.

[18] Y. Gao, S. Chen, D. Cao, G. Wang, and J. Yin, "Electrochemical capacitance of Co_3O_4 nanowire arrays supported on nickel foam," *Journal of Power Sources*, vol. 195, no. 6, pp. 1757–1760, 2010.

[19] L. Wang, X. Liu, X. Wang, X. Yang, and L. Lu, "Preparation and electrochemical properties of mesoporous Co3O4 crater-like microspheres as supercapacitor electrode materials," *Current Applied Physics*, vol. 10, no. 6, pp. 1422–1426, 2010.

[20] W. Liu, D. Jiang, J. X. Xia, J. Qian, K. Wang, and H. M. Li, "Preparation of hierarchical mesoporous Co3O4 bundle using [Bmim]TA as a multi-role starting material and its supercapacitor application," *Monatshefte fur Chemie*, vol. 145, no. 1, pp. 19–22, 2014.

[21] R. Tummala, R. K. Guduru, and P. S. Mohanty, "Nanostructured Co_3O_4 electrodes for supercapacitor applications from plasma spray technique," *Journal of Power Sources*, vol. 209, no. 7, pp. 44–51, 2012.

[22] G.-L. Zhang, D. Zhao, P.-Z. Guo, Z.-B. Wei, and X.-S. Zhao, "Glycerol-assisted synthesis and electrochemical properties of Co3O4 nanowires," *Acta Physico—Chimica Sinica*, vol. 28, no. 2, pp. 387–392, 2012.

[23] M. Chowdhury, O. Oputu, M. Kebede et al., "Rapid and large-scale synthesis of Co_3O_4 octahedron particles with very high catalytic activity, good supercapacitance and unique magnetic properties," *RSC Advances*, vol. 5, no. 127, pp. 104991–105002, 2015.

[24] D. Wang, Q. Wang, and T. Wang, "Morphology-controllable synthesis of cobalt oxalates and their conversion to mesoporous Co_3O_4 nanostructures for application in supercapacitors," *Inorganic Chemistry*, vol. 50, no. 14, pp. 6482–6492, 2011.

[25] L. Tao, L. Shengjun, Z. Bowen et al., "Supercapacitor electrode with a homogeneously Co_3O_4-coated multiwalled carbon nanotube for a high capacitance," *Nanoscale Research Letters*, vol. 10, no. 1, pp. 1–7, 2015.

[26] H. Wang, Y. Shi, Z. Li, W. Zhang, and S. Yao, "Synthesis and electrochemical performance of Co3O4/graphene," *Chemical Research in Chinese Universities*, vol. 30, no. 4, pp. 650–655, 2014.

[27] Z. Hai, L. Gao, Q. Zhang et al., "Facile synthesis of core-shell structured PANI-Co3O4 nanocomposites with superior electrochemical performance in supercapacitors," *Applied Surface Science*, vol. 361, pp. 57–62, 2016.

[28] V. G. Hadjiev, M. N. Iliev, and I. V. Vergilov, "The Raman spectra of Co_3O_4," *Journal of Physics C: Solid State Physics*, vol. 21, no. 7, pp. L199–L201, 1988.

[29] G. Wang, X. Shen, J. Horvat et al., "Hydrothermal synthesis and optical, magnetic, and supercapacitance properties of nanoporous cobalt oxide nanorods," *Journal of Physical Chemistry C*, vol. 113, no. 11, pp. 4357–4361, 2009.

[30] Y.-Z. Zhang, Y. Wang, Y.-L. Xie et al., "Porous hollow Co3O4 with rhombic dodecahedral structures for high-performance supercapacitors," *Nanoscale*, vol. 6, no. 23, pp. 14354–14359, 2014.

[31] K. Qiu, H. Yan, D. Zhang et al., "Hierarchical 3D mesoporous conch-like Co3O4 nanostructure arrays for high-performance supercapacitors," *Electrochimica Acta*, vol. 141, pp. 248–254, 2014.

[32] H. Wei, C. He, J. Liu et al., "Electropolymerized polypyrrole nanocomposites with cobalt oxide coated on carbon paper for electrochemical energy storage," *Polymer*, vol. 67, pp. 192–199, 2015.

[33] K. Ling Bin, L. Yu Gang, L. Mao Cheng, L. Yong Chun, and K. Long, "Preparation and supercapacitiveproperties evaluation of Co_3O_4 nanoparticles," *Applied Chemical Industry*, vol. 41, no. 1, pp. 102–105, 2012.

[34] Z. Wei Zhuo and H. Su Kun, "Crystal growth habits and formation mechanism," in *Crystal Growth Morphology*, pp. 277–355, 1999.

[35] W. Liu, X. Li, M. Zhu, and X. He, "High-performance all-solid state asymmetric supercapacitor based on Co3O4 nanowires and carbon aerogel," *Journal of Power Sources*, vol. 282, pp. 179–186, 2015.

[36] Y. W. Liu, C. Y. Zhang, W. W. Zhao et al., "Electrochemical capacitance characteristics of corn-like Co_3O_4 nanorods prepared by solvothermal method," *Journal of China Three Gorges University (Natural Science)*, vol. 34, no. 5, pp. 103–107, 2012.

[37] B. Gnana Sundara Raj, A. M. Asiri, J. J. Wu, and S. Anandan, "Synthesis of Mn_3O_4 nanoparticles via chemical precipitation approach for supercapacitor application," *Journal of Alloys and Compounds*, vol. 636, no. 7, pp. 234–240, 2015.

[38] F. Lu, Y. Ru Fu, and X. Yan, "The preparation of flake-like cobalt oxide and its electrical performance," *Journal of Huangshan University*, vol. 17, no. 3, pp. 46–49, 2015.

[39] C. Cao and J. Zhang, "An introduction to electrochemical impedance spectroscopy," 2002.

[40] S. Wen and Z. Ping, "Preparation of the honeycomb-shaped Co_3O_4 and its supercapacitor performance," *Micronanoelectronic Technology*, vol. 53, no. 3, pp. 201–204, 2016.

[41] Q. Huang, Y. Dai, H. Zhang, W. Wang, and Y. Chen, "Preparation and capacitance performance of Co_3O_4 nanocluster arrays," *Fine Chemicals*, vol. 33, no. 1, pp. 19–23, 2016.

[42] F. Zhang, L. Hao, L. Zhang, and X. Zhang, "Solid-state thermolysis preparation of Co3O4 nano/micro superstructures from metal-organic framework for supercapacitors," *International Journal of Electrochemical Science*, vol. 6, no. 7, pp. 2943–2954, 2011.